Supporting Information for:

Investigating the Dynamics of Destabilized Nucleosomes Using Methyl-TROSY NMR

Julianne L. Kitevski-LeBlanc[1]*, Tairan Yuwen[1], Pamela N. Dyer[2], Johannes Rudolph[2], Karolin Luger[2,3] and Lewis E. Kay[1,4]*

[1]Departments of Chemistry, Molecular Genetics, and Biochemistry, University of Toronto, Toronto, Ontario M5S 1A8, Canada, [2]Department of Chemistry and Biochemistry, University of Colorado, Boulder, CO 80309, United States, [3]Howard Hughes Medical Institute, and [4]Program in Molecular Medicine, Hospital for Sick Children, 555 University Avenue, Toronto, Ontario M5G 1X8, Canada

SI Materials and Methods

Protein expression and purification

D. melanogaster histone genes for H2A, H2B, H3 and H4 were cloned into a pET21b expression vector, as described previously[1]. All mutants including H3A98H, H4Y98H, and H4Y98W were prepared with PfuTurbo DNA polymerase using the QuikChange site-directed mutagenesis method (Strategene). Protein expression was achieved by growing *E. coli* BL21(DE3) cells at 37°C, transformed with the desired expression plasmid, in media containing 100 mg/L ampicillin. Expression was induced with 1mM IPTG for 16 hours at 37°C for H2A, H2B and H3 and 4 hours at 37°C for H4. Cells were subsequently harvested by centrifugation and purified immediately or stored at -80°C. Deuterated histones were expressed in 99.9% D_2O minimal M9 media supplemented with 3 g/L [^{2}H,^{12}C]-glucose. For the expression of H2B with Ileδ1-[$^{13}CH_3$] and Leu/Val-[$^{13}CH_3$,$^{12}CD_3$] methyl labeling (ILV-methyl labeling)[2], 99.9% D_2O minimal M9 media was supplemented with 3 g/L [^{2}H,^{12}C]-glucose, 85 mg/L α-ketoisovaleric acid (L/V labeling) and 45 mg/L α-ketobutyric acid (I labeling) one hour prior to induction of protein overexpression. All histones were purified from inclusion bodies using HighTrap SP-XL ion exchange columns (GE Healthcare) equilibrated in 7 M urea, 150 mM NaCl, 50 mM Tris pH 8 and eluted using a linear gradient up to 1 M NaCl over 9 column volumes. Fractions containing the histone proteins were then pooled, concentrated and further purified using a HighLoad 10/300 S75 superdex gel filtration column (GE Healthcare), followed by extensive dialysis into water and lyophilization. Protein purity was evaluated using SDS-PAGE and electrospray ionization-mass spectrometry (ESI-MS).

DNA preparation

153-bp 601 DNA[3] was prepared from a 32-copy plasmid (a gift from Dr. Tom Muir's lab), transformed into DH5α *E. coli* cells and grown overnight in LB media supplemented with 100 mg/L ampicillin at 37°C. Following harvest by centrifugation, Giga prep plasmid purification kits (Qiagen, cat.12191) were used to purify the 32-copy plasmid. Digestion using EcoRV (0.5 units/μg plasmid) in NEB buffer3 (10 mM $MgCl_2$, 50 mM Tris-HCL, 1 mM DTT, 100 mM NaCl, pH 7.9) was carried out for 20 hours at 37°C. The resulting solution of liberated 153-bp fragments was treated with 0.3375 volume equivalents of fresh 40% PEG-600 and 0.15 volume equivalents of 5 M NaCl solution and incubated at 4°C for 1 hour to precipitate the vector backbone. Following centrifugation at 14,000 rpm for 30 minutes at 4°C, 2.5 volume equivalents of 100% ethanol was added to the supernatant and left at -20°C overnight to precipitate the 153-bp 601 DNA fragments. Following centrifugation at 14,000 rpm for 30 minutes at 4°C, the precipitated DNA pellet was washed once with cold 70% ethanol and resuspended in 10 mM Tris pH 8. The 153-bp 601 DNA fragments were further purified using a HiTrap DEAE-FF column (GE Healthcare) equilibrated in 10 mM Tris pH 8 and eluted using a linear gradient up to 1 M KCl over 9 column volumes. Fractions containing DNA were pooled, concentrated and the final concentration of KCl was adjusted to 2 M for subsequent NCP reconstitution.

Octamer refolding and NCP reconstitution

Purified H2A, H2B, H3(or H3A98H), and H4(or H4Y98H, H4Y98W) were combined in equimolar ratios and refolded into octamers (WT H4 and H4Y98W) or separately into dimer and tetramers (H4Y98H and H3A98H/H4Y98H), which were subsequently

purified and reconstituted into NCPs as previously described[4]. Microscale test NCP reconstitution reactions (50 μL, 7 μM DNA) were used to determine the optimal stoichiometry of octamers (WT and H4Y98W) or dimer/tetramer (H4Y98H and H3A98H/H4Y98H) and (601 or 5S rRNA) DNA. Following reconstitution, NCPs prepared with 5S rRNA DNA were exchanged into 10 mM Tris pH 7.5 buffer by dialysis and heat shifted at 37°C for 1 hour to obtain a single, symmetrically wrapped NCP particle. The quality and purity of the resulting NCPs were checked using 7% native PAGE.

NMR experiments

All NMR experiments were performed at 45°C using 14.0 and 18.7 T Bruker Avance III HD spectrometers equipped with cryogenically cooled pulse-field gradient triple-resonance probes, unless specified otherwise. The NMR buffer contained 0.05% azide and 20 mM sodium phosphate pH 6, in 99.9% D_2O. Sample concentrations were in the range of 50-150 μM in NCP, as determined by A260 measurement of DNA. All NMR data were processed and analyzed using the suite of programs provided in NMRPipe/NMRDraw and NMRviewJ software packages[5,6].

^{1}H-^{13}C HMQC spectra of ILV-methyl labeled H2B NCPs were recorded, exploiting the methyl-TROSY effect to obtain high quality spectra[7]. Assignments of all ILV methyl resonances of H2B were transferred from those previously published[1].

Translational diffusion coefficients were measured by recording a series of 1D ^{13}C-edited spectra at 25°C using a pulse sequence analogous to an ^{15}N-edited experiment published previously[8], with 9 gradient strengths ranging from 4.5 to 40.5 G/cm. After

initial gradient encoding of the magnetization a constant-delay diffusion element of 250 ms for NCPs (~210 kDa) and the ¼ proteasome (180 kDa) was employed and the net duration of encoding/decoding gradients was 2 ms. The resulting ^{1}H methyl signal was integrated to quantify peak intensities as a function of gradient strength. Diffusion constants were obtained by nonlinear least square fits of methyl signal intensities as a function of the square of the gradient strength according to the relation $I = I_o\exp(-aDG^2)$ where I and I_o are the integrated peak intensities in the presence and absence of the gradient G, respectively, D is the diffusion constant and a is a constant comprised of experimental parameters.

Transverse relaxation (R_2) rates for the slowly relaxing component of methyl proton magnetization were measured as previously described[9], at 45°C 14.0T. The relaxation delays (T) used were 2, 4, 7, 9, 11, 13, 15 and 17 ms. Rates were obtained by fitting peak intensities to a single exponential decay function, $y=A\exp(-R_2T)$, with errors estimated from Monte Carlo analysis[10].

Methyl ^{1}H,^{13}C multiple-quantum CPMG data sets were recorded at 45°C, 14.0 and 18.7T, using a previously published pulse scheme[11]. A relaxation delay of 18 ms (T_{CPMG}) afforded the collection of 18 CPMG pulse frequencies (ν_{CPMG}) ranging from 56 – 2000 Hz with two duplicate points to assess experimental errors. Peak intensities were used to calculate effective relaxation rates ($R_{2,eff}$) for each CPMG frequency according to the relation $R_{2,eff} = (-1/T_{CPMG})\ln(I/I_o)$, where I and I_o are peak intensities measured with and without the CPMG delay. The variation in $R_{2,eff}$ with ν_{CPMG} was fit to a two-state model of chemical exchange ($G \underset{k_{EG}}{\overset{k_{GE}}{\rightleftharpoons}} E$, where G and E are ground and excited states,

respectively) based on the Bloch-McConnell equations[12], to extract values of exchange parameters (p_E, k_{ex}=k_{GE}+k_{EG}), as well as ^{1}H and ^{13}C chemical shift differences for nuclei interconverting between pairs of states. In-house written software (ChemEx, https://github.com/gbouvignies/chemex) was used for this analysis. Global fits included 8 profiles for H4Y98H and H3A98H/H4Y98H NCPs at pH 6 (V45γ2, I58δ1, I66δ1, L77δ2, L97δ1, L98δ1/δ2, and L99a), 6 profiles for H3A98H/H4Y98H at pH 7.5 (I58δ1, I66δ1, L77δ2, L98δ1/δ2, and L99a) and 7 profiles for H3A98H/H4Y98H NCPs with 5S rRNA DNA (V45γ2, I58δ1, I66δ1, L97δ1, L98δ1/δ2, and L99a).

χ^2 surface plots were generated for each NCP sample to evaluate the robustness of the extracted exchange parameters (p_E, k_{ex}). Numerical fitting was performed using the ChemEx program as before, with p_E and k_{ex} sampled from a grid with values ranging from 0-30% and 0-3000 s^{-1}, respectively. The χ^2 surface was prepared using two different strategies. In the first method, $|\Delta\varpi|$ was free to change during the χ^2 minimization procedure for each set of (p_E, k_{ex}). In the second method, chemical shift differences were fixed to those obtained from a global fit that included the four NCP samples used in this study. In this case ^{13}C (^{1}H) $|\Delta\varpi|$ values were: V45γ2: 0.24 ± 0.01 ppm (0.054 ± 0.026 ppm); I58δ1: 0.95 ± 0.04 ppm (0.130 ± 0.003 ppm); I66δ1: 1.38 ± 0.05 ppm (0.135 ± 0.003 ppm); L77δ2: 1.02 ± 0.04 ppm (0.087 ± 0.007 ppm); L97δ2: 0.49 ± 0.03 ppm (0.099 ± 0.011 ppm); L98δ1: 0.26 ± 0.01 ppm (0.072 ± 0.017 ppm); L98δ2: 0.58 ± 0.02 ppm (0.076 ± 0.004 ppm); and L99a: 0.38 ± 0.01 ppm (0.093 ± 0.004 ppm). All other parameters such as $R_{2,G}$ and ΔR_2 (=$R_{2,E}$ − $R_{2,G}$), where $R_{2,G}$ and $R_{2,E}$ are intrinsic

transverse relaxation rates for nuclei in the ground and excited states, respectively, were free to change during minimization of χ^2 for a given set of (p_E, k_{ex}).

Thermodynamic competition assays

For each titration point 5 nM WT or mutant NCP wrapped with Alexa Fluor 488-labeled 147-bp 601 DNA was mixed with 147-bp 601[3] competitor DNA ranging in concentration from 0.08 to 10 μM for WT and H4Y98W NCPs, and from 0.04 to 3 μM for H4Y98H and H3A98H/H4Y98H NCPs. The reaction buffer contained 20 mM MES pH 6.0, 150 mM NaCl, 1 mM EDTA, 1 mM DTT and 0.01% Nonident P-40. Reactions were incubated at room temperature overnight in the dark and then analyzed on a 5% polyacrylamide mini-gel in 0.2X TBE buffer at 150 volts for 70 minutes, 4˚C. The gel was scanned using a Typhoon FLA 9500 instrument and the nucleosome bands quantitated with ImageQuantTL. Non-linear regression analysis of the data was performed to obtain IC50 values for the removal of histones from the NCPs using the following equation,

$$y = I_{\min} + \frac{I_{\max} - I_{\min}}{(1+10^{(\log_{10} \mathrm{IC50} - x)n})} \qquad [1]$$

where I_{max} and I_{min} are the maximum and minimum NCP band intensities corresponding to no added competitor DNA or the addition of an infinitely high concentration, respectively, IC50 is the concentration of competitor DNA where the NCP band intensity is reduced by 50%, x is the $\log_{10}$ of the added concentration of DNA and n, is the Hill-slope (<0).

The identity of tetrasome, hexasome and NCP species on 5% native PAGE gels

was confirmed using a differential fluorescent labeling approach (Fig. S2C). Specifically, tetramers were labeled with Alexa-488 via attachment to H3, while dimers were labeled with Atto-647 via attachment to H2B, as described previously[13]. Combining labeled tetramers, dimers and 147 bp 601 DNA in equal ratios produces a mixture of the three species, with the formation of NCP (and hexasome) species confirmed by FRET between dimer and tetramers. Adding an additional equivalent of dimer promotes the formation of NCPs, allowing for the identification of hexasomes from depletion of this species in comparison to equal stoichiometric mixtures. Tetramers are easily assigned by combination of labeled tetramer and 147 bp DNA alone.

Calculation of relative stabilities of NCPs

As described above, methyl ^{1}H,^{13}C multiple-quantum CPMG data sets were fit to a two-site exchange model so as to extract (p_E, k_{ex}) values as well as ^{1}H and ^{13}C chemical shift differences for nuclei exchanging between the two states. For a given NCP the free energy difference between exchanging states is $\Delta G_{GE} = G_E - G_G = -RT\ln(\frac{p_E}{p_G})$ where p_E=1-p_G, T is the temperature in K and R is the gas constant. Assuming that the change to the stability of the NCP derives from changes to the ground state free energy exclusively then the ground state of mutant j is elevated in free energy with respect to the WT by

$$\Delta G_{WT,j} = G_{G,j} - G_{G,WT} = -RT\{-\ln(\frac{p_E^j}{p_G^j}) + \ln(\frac{p_E^{WT}}{p_G^{WT}})\}. \quad [2]$$

For the WT NCP $p_E \leq 1\%$ based on the results of Figure S6, with values of p_E = 8.2±0.5% and 15.6±1.4% for H4Y98H and H3A98H/H4Y98H NCPs, respectively (Figure S5).

SI Text

Comparison of NMR-observed excited state with alternative NCP conformations

A recent cryo-EM study highlights a series of WT NCPs with DNA and histone conformations that are distinct from those observed in crystal structures[14]. The structures exhibit varying amounts of asymmetric DNA unwrapping, including a bulge near one DNA entry/exit point, asymmetric unwrapping of ~15 base pairs (bps), as well as several structures with more than 40 bps unwrapped, resulting in the loss of map density for the proximal H2A-H2B dimer. Although it is not possible to obtain a detailed structure of the excited state observed in the present study via the methyl-TROSY CPMG relaxation dispersion approach that we have exploited, it is possible, however, to present arguments about whether the state observed by NMR is likely to be similar to one or more of those characterized via cryo-EM. In their analysis of a pair cryo-EM structures, focusing on one that is essentially identical to the X-ray model and a second with unwrapping of ~15 bps of DNA, Bilokapic et al.[14] observed significant changes for helices near the DNA entry/exit point, including H3 αN, H2A α2 and α3, and H2B α1 and α2. Recall that our NMR study focuses on methyl probes within H2B that can serve as reporters for changes in structure. There are several methyl probes within H2B α1, namely, I36, I38, V41, L42, and V45, as well as I51 in loop 1, with nearest distances to DNA in the range of 4 – 20 Å that can be used to test the hypothesis that the excited state structure observed by NMR corresponds to one where bps from one end of the DNA have unwound. In this regard, the closest methyl probes to DNA include those from I36 and I51, which have flat dispersion profiles in all of the NCPs studied, suggesting that this region does not undergo any structural rearrangement in forming the excited state characterized here. In

contrast, large dispersion profiles were observed for methyl groups of residues localized to the dimer-tetramer interface, with the largest measured for L77δ2. A nearby probe, I86, which sits closer to DNA than L77δ2, has a flat dispersion profile and, in general, we find a poor correlation between proximity to DNA and dispersion profile size, arguing against a DNA unwrapping event as the source of the 'NMR' excited state. Further, as discussed in the text, there is a steep pH dependence to the population of the NMR excited state that is correlated to the ionization state of histidine residues; such a pH profile would not be expected for a mechanism involving unraveling of DNA exclusively.

It is worth emphasizing that the lack of evidence for the novel conformations observed in cryo-EM in our study does not imply that these unique structures are not present in solution, at least to some extent. The observation of sparsely populated, transiently formed states via CPMG relaxation dispersion requires fractional populations of > ~0.5% for the rare states and exchange rates ranging between several hundreds to several thousands per second[15]. In addition, chemical shift differences between spins in each of the interconverting states must be different, often implying significant structural changes. Further, the flat dispersion profiles observed for the WT NCP do not necessary imply that the excited state characterized for the H3A98H/H4Y98H and H4Y98H NCPs is not present in the WT system. However, as indicated in Figure S6, the population of the excited state is most likely reduced below the detection point for the WT NCP so that the dynamics, if present, escape detection.

Comparison of dynamics of octamers prepared with 5S rRNA- and 601-DNA

Our study of H3A98H/H4Y98H octamers prepared with either 5S rRNA or 601 DNA sequences revealed no significant changes in measured dispersion profiles nor, therefore, in fitted exchange rates, populations and $|\Delta\varpi|$ values, despite the significant difference in NCP stabilities previously measured for these two DNA fragments[3]. This may be attributed to the conditions of our experiments, as low salt and high NCP concentrations favor fully wrapped, stable NCPs. As mentioned above, there are many methyl probes in H2B that could be sensitive to changes in DNA, subject of course to the limitations of the CPMG method discussed above. In this regard it seems likely that the stability of the 5S rRNA DNA complex remains sufficiently high, despite a 3 kcal/mol decrease relative to 601 complexes, so that excited state populations resulting from potentially increased DNA breathing in the 5S NCP remain under the detection limit for the CPMG method. However, a comparison of HMQC spectra of the two complexes did establish some changes. For example, weak secondary peaks were observed for I66 for both 5S and 601 NCPs; the peak for the 5S NCP was 5 fold higher (relative to the primary I66 peak). Additionally, a second peak was observed only for V45γ2 in the 5S NCP. These spectral features indicate subtle differences in the two classes of NCP studied here.

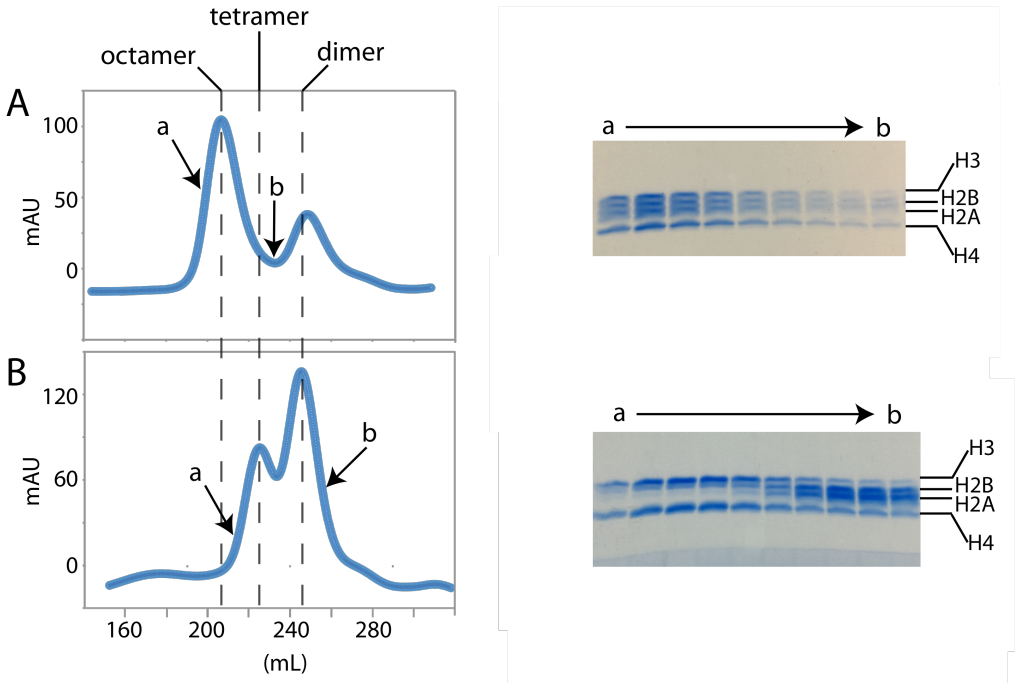

Figure S1. Representative gel filtration purification chromatograms of WT (A) and H4Y98H (B) octamers, with associated SDS page analysis shown to the right. Standard elution volumes for octamer (~207 mL), tetramer (~222 mL) and dimer (~242 mL) are indicated with dashed lines, and labeled at top. SDS page analysis sampled elution fractions between points 'a' and 'b', as indicated in each chromatogram. Band migration for histones indicated along right edge of gels.

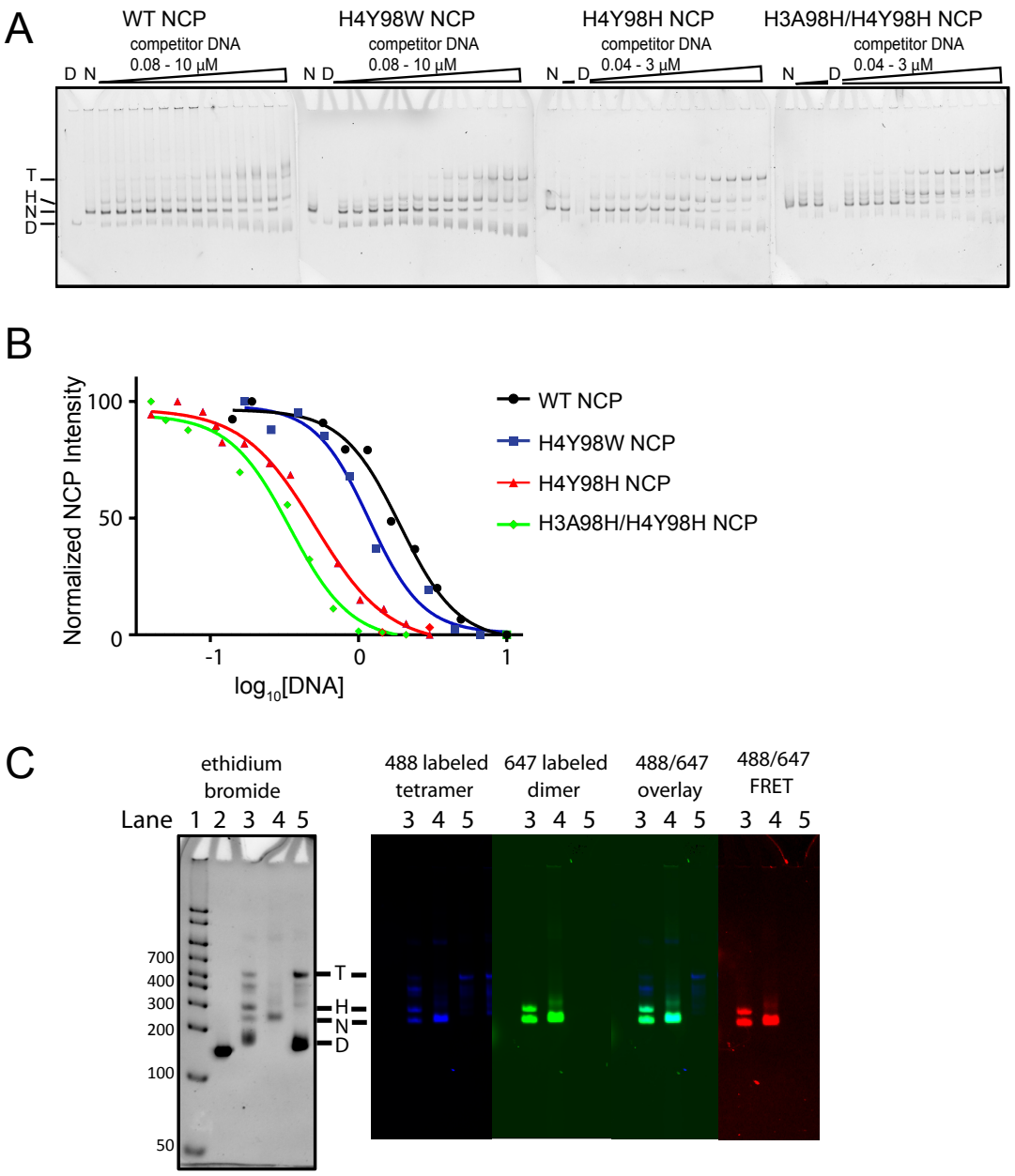

Figure S2. (A) Representative 5% native PAGE gel of a DNA competition assay to establish relative nucleosome stabilities. Migrations of NCP (N), hexasome (H, nucleosome lacking one H2A-H2B dimer), tetrasome (T, $(H3\text{-}H4)_2$ tetramer bound to DNA) and (D) free DNA are indicated at far left. The identity of the NCP used in each gel, as well as the range of competitor DNA employed is indicated. In some gels, the titration series is interrupted by a control lane containing free DNA (D). (B) Experimental data (points) and best fits (lines) from non-linear regression analysis of normalized NCP band intensity (lane N in A) as a function of $\log_{10}$ of competitor DNA added (in μM). (C) 5% native PAGE gel for assignment of tetrasome (T), hexasome (H) and NCP (N) species using Alexa-488 labeled tetramers and Atto-647 labeled dimers. The stain (ethidium bromide) or fluorescent dye visualized in each image is indicated with lanes identified along the top edge. Lane 1: DNA molecular weight marker; Lane 2: 147 bp

DNA; Lane 3: 1:1:1 mixture of tetramer:dimer:147 bp DNA; Lane 4: 1:2:1 mixture of tetramer:dimer:147 bp DNA; Lane 5: 1:1 mixture of tetramer:147 bp DNA. Lane 3 shows a mixture of tetrasomes, hexasomes and NCP. A higher ratio of dimer (Lane 4) promotes the formation of NCPs, depleting the hexasome band intensity and thus providing its assignment. Lane 5 confirms the identity of tetrasomes (only H3/H4 and DNA added). FRET between labeled dimers and tetramers provides unambiguous identification of NCP and hexasomes.

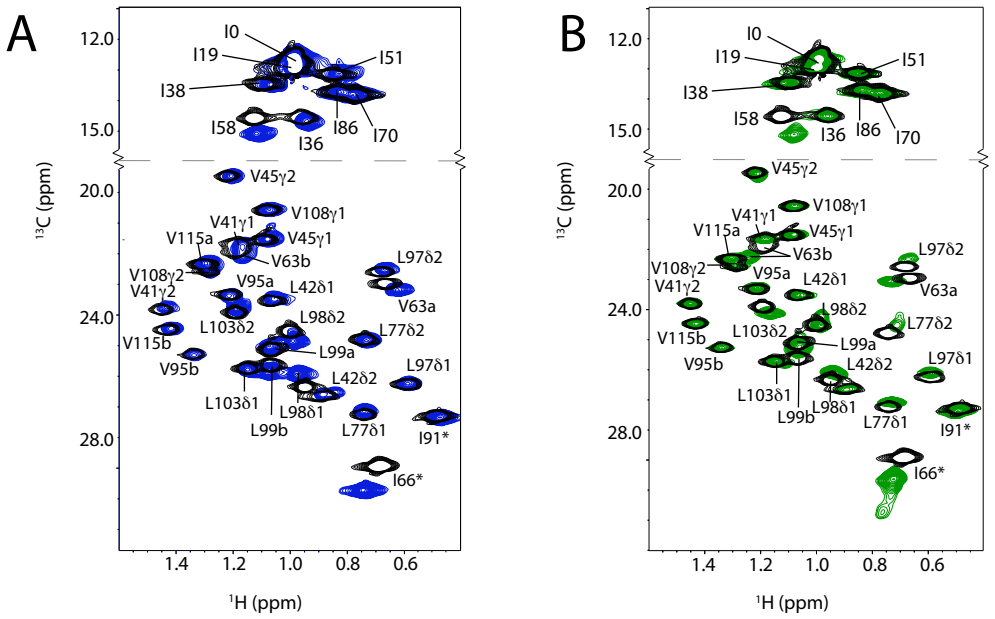

Figure S3. Overlay of ^{1}H-^{13}C HMQC spectra of ILV-methyl labeled H2B NCPs, WT (black) with H4Y98W (blue) (A) and WT with H4YA98H/H3A98H (green) (B) collected at 18.7T, 45°C. Aliased peaks denoted with *, and assignments as indicated.

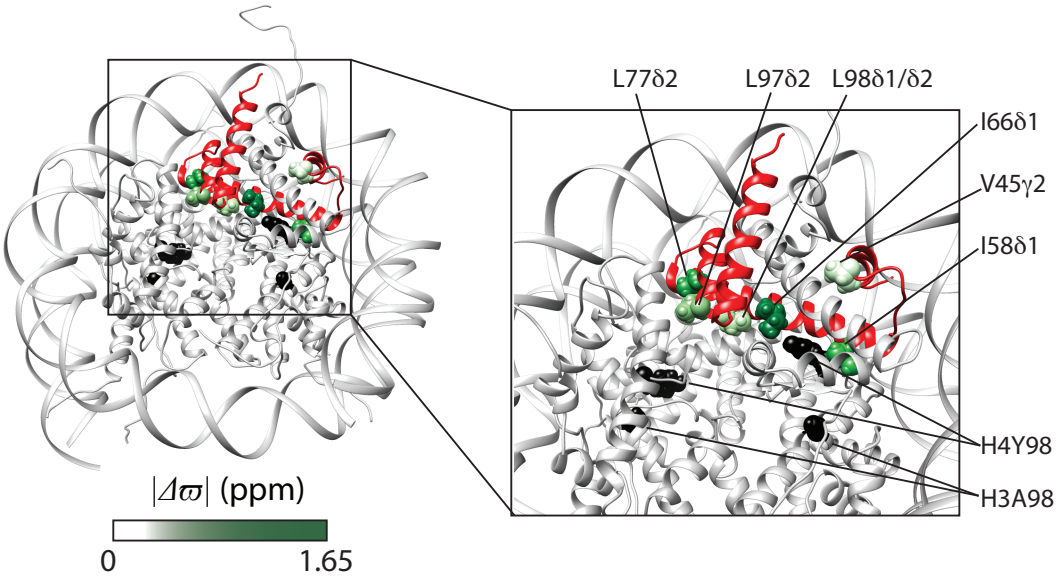

Figure S4. Distribution of methyl probes with non-flat CPMG dispersion profiles mapped onto the *D. melanogaster* crystal structure (2PYO). The location of point mutations H3A98H and H4Y98(H or W) are shown in space filling representation, and colored black. Methyl probes for which CPMG dispersions were fit are shown within one H2B polypeptide chain (red), in space filling representation and colored green according to the magnitude of $|\Delta\varpi|$ values. All other histones and DNA are colored grey.

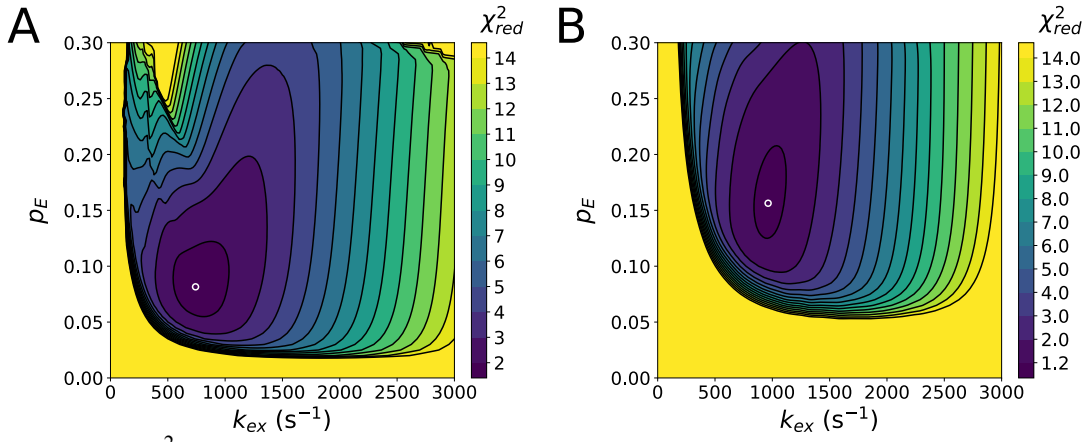

Figure S5. χ^2 surface plots generated from fits of CPMG relaxation dispersion data recorded at 14.0 and 18.7T on ILV-methyl labeled H2B NCP samples, H4Y98H (A) and H3A98H/H4Y98H at pH 6 (B). The $|\Delta\varpi|$ values were not fixed during the search for the minimum χ^2 value. The white circle in each plot indicates the position of (p_E,k_{ex}) that corresponds to the global minimum of χ^2. Values of (p_E,k_{ex})=(8.2±0.5%,742±30s^{-1}), (15.6±1.4%,963±33s^{-1}) were obtained in A and B, respectively, corresponding to χ^2 values of 1.6 and 1.1.

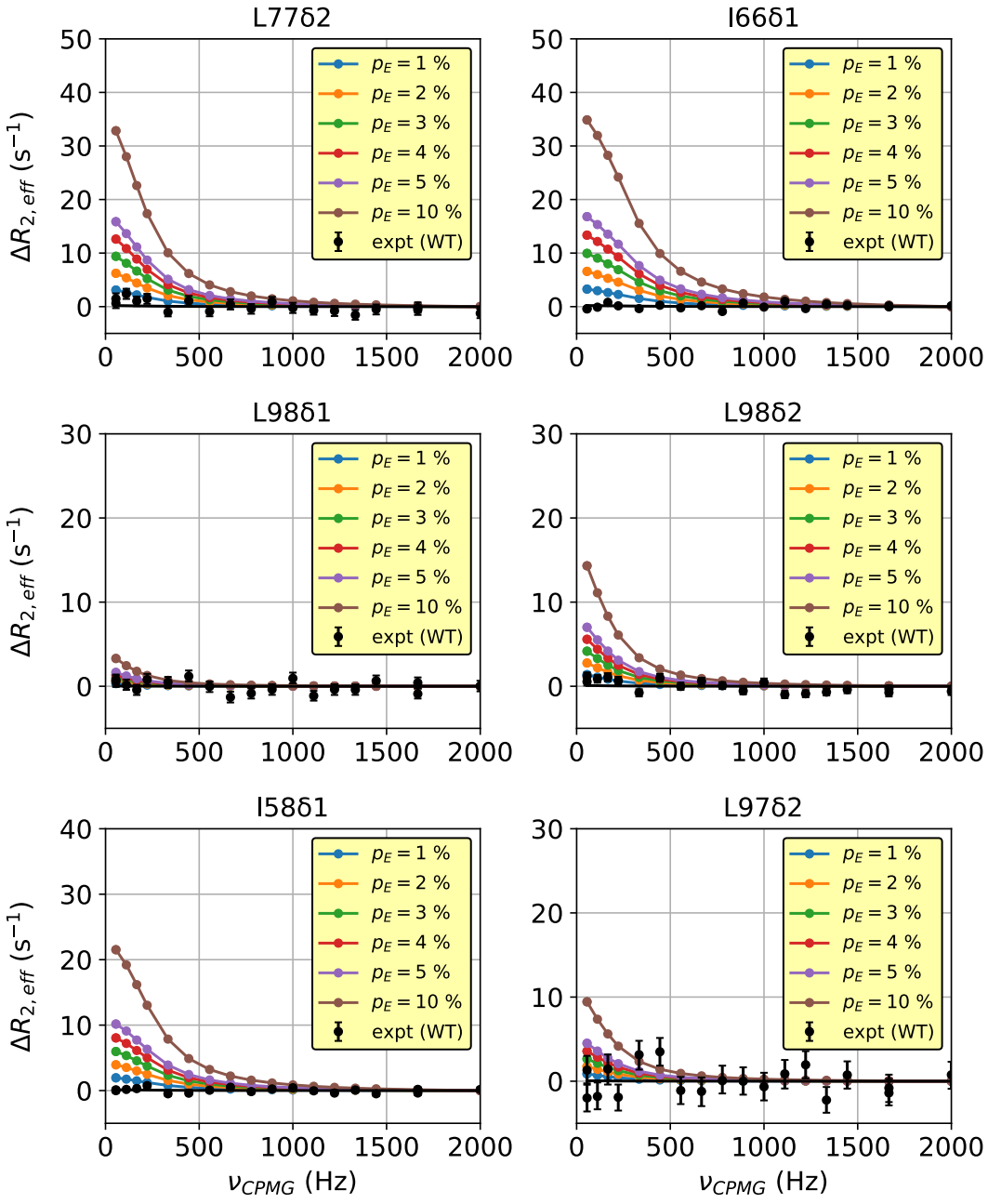

Figure S6. Simulated CPMG relaxation dispersion profiles for selected Ile and Leu H2B residues using $|\Delta\varpi|$ (both ^{13}C and ^{1}H) and k_{ex} (963 s^{-1}) values that were obtained from fits of experimental data, as a function of p_E. Experimental profiles for the WT NCP are also shown (black). $\Delta R_{2,eff} = R_{2,eff}(\nu_{CPMG}) - R_{2,eff}(\nu_{CPMG}$=2000Hz) values are plotted. It is clear that for the WT NCP $p_E \leq 1\%$ and thus a value of 1% was used to calculate the minimum ΔG between ground and excited states in this case.

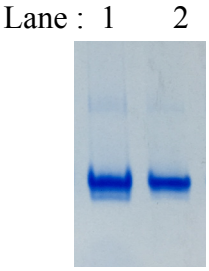

Figure S7. 7% native polyacrylamide gel of H3A98H/H4Y98H octamers wrapped with 5S rRNA DNA (Lane 1) and 601 DNA (Lane 2). The gel was run in 1X Tris/Borate/EDTA buffer, pH 8 at 150 volts, 4°C for 1.5 hours, followed by protein staining using 0.1% Coomassie blue.

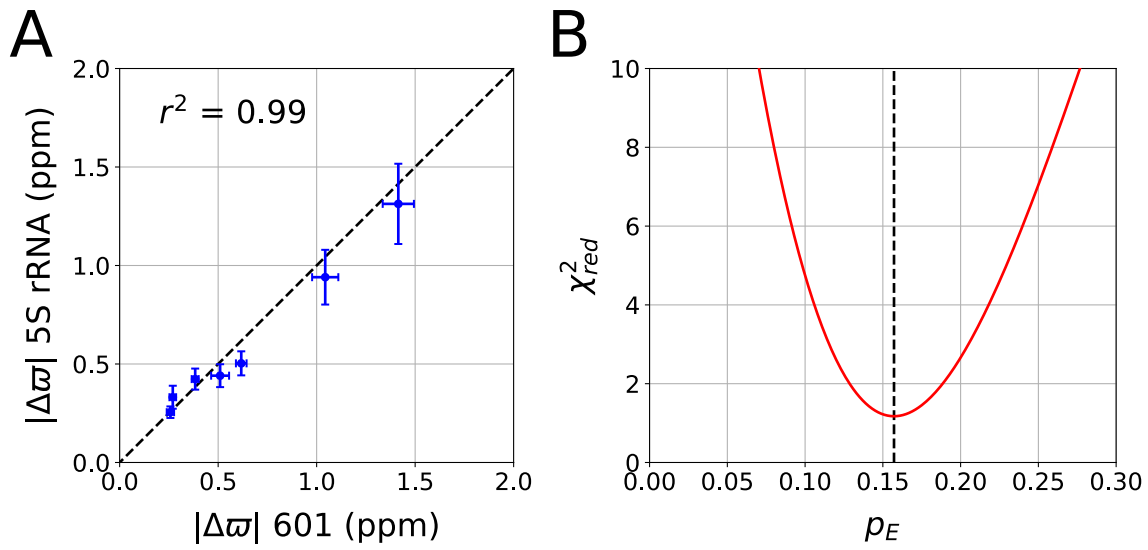

Figure S8. A. Correlation of ^{13}C $|\Delta\varpi|$ values obtained from fits of methyl-TROSY CPMG data recorded on NCP samples with the H3A98H/H4Y98H mutations prepared with either 601 or 5S rRNA DNA. Dispersion profiles from separate NCPs were fit independently. B. Corresponding 1D χ^2 surface plot of the resultant goodness of fit of dispersion data recorded on the H3A98H/H4Y98H NCP prepared with 5S rRNA DNA (pH 6). The value of k_{ex} was fixed to that obtained for the global minimum of χ^2, with p_E varied as indicated. Values of $|\Delta\varpi|$ were held to those obtained from a global fit of all data sets recorded on all NCP samples, as described in the Material and Methods section. The dashed line indicates the position of p_E that corresponds to the global minimum of χ^2.

NCP	IC50 (μM), pH 6
WT	1.8 ± 0.2
H4Y98W	1.6 ± 0.2
H4Y98H	0.6 ± 0.1
H3A98H/H4Y98H	0.4 ± 0.1

Table S1. Summarized results from fluorescence-based competitive DNA assay. IC50 values were obtained from non-linear regression analysis of NCP DNA band intensities quantified from 5% native PAGE gel analysis.

References

(1) Kato, H.; van Ingen, H.; Zhou, B. R.; Feng, H. Q.; Bustin, M.; Kay, L. E.; Bai, Y. W. *Proc. Natl. Acad. Sci. U. S. A.* **2011**, *108*, 12283.

(2) Tugarinov, V.; Kay, L. E. *J. Biomol. NMR* **2004**, *28*, 165.

(3) Lowary, P. T.; Widom, J. *J. Mol. Biol.* **1998**, *276*, 19.

(4) Dyer, P. N.; Edayathumangalam, R. S.; White, C. L.; Bao, Y.; Chakravarthy, S.; Muthurajan, U. M.; Luger, K. *Methods Enzymol.* **2004**, *375*, 23.

(5) Delaglio, F.; Grzesiek, S.; Vuister, G. W.; Zhu, G.; Pfeifer, J.; Bax, A. *J. Biomol. NMR* **1995**, *6*, 277.

(6) Johnson, B. A.; Blevins, R. A. *J. Biomol. NMR* **1994**, *4*, 603.

(7) Tugarinov, V.; Hwang, P. M.; Ollerenshaw, J. E.; Kay, L. E. *J. Am. Chem. Soc.* **2003**, *125*, 10420.

(8) Choy, W. Y.; Mulder, F. A. A.; Crowhurst, K. A.; Muhandiram, D. R.; Millett, I. S.; Doniach, S.; Forman-Kay, J. D.; Kay, L. E. *J. Mol. Biol.* **2002**, *316*, 101.

(9) Tugarinov, V.; Kay, L. E. *J. Am. Chem. Soc.* **2006**, *128*, 7299.

(10) Press, W. H., Flannery, B., P., Teukolsky, S., A., Vetterling, W., T. *Numerical Recipies in C*; Cambridge University Press: Cambridge, UK, 1998.

(11) Korzhnev, D. M.; Kloiber, K.; Kanelis, V.; Tugarinov, V.; Kay, L. E. *J. Am. Chem. Soc.* **2004**, *126*, 3964.

(12) McConnell, H. M. *J. Chem. Phys.* **1958**, *28*, 430.

(13) Muthurajan, U.; Mattiroli, F.; Bergeron, S.; Zhou, K.; Gu, Y.; Chakravarthy, S.; Dyer, P.; Irving, T.; Luger, K. *Methods Enzymol.* **2016**, *573*, 3.

(14) Bilokapic, S.; Strauss, M.; Halic, M. *Nat. Struct. Mol. Biol.* **2018**, *25*, 101.

(15) Palmer, A. G.; Kroenke, C. D.; Loria, J. P. *Methods Enzymol* **2001**, *339*, 204.